Supplementary Digital Content to:

The role of Nav1.7 in human nociceptors: insights from human iPS cell-derived sensory neurons of erythromelalgia patients

Jannis E. Meents*[1], Elisangela Bressan*[1#], Stephanie Sontag*[2,3#], Alec Foerster*[1], Petra Hautvast[1], Corinna Rösseler[1], Martin Hampl[1,4], Herdit Schüler[5], Roman Goetzke[6], Thi Kim Chi Le[1], Inge Petter Kleggetveit[7], Kim Le Cann[1], Clara Kerth[1], Anthony M. Rush[8], Marc Rogers[8], Zacharias Kohl[9], Martin Schmelz[10], Wolfgang Wagner[2,6], Ellen Jørum[7,11], Barbara Namer[4,12], Beate Winner[13,14], Martin Zenke[2,3], Angelika Lampert[1]

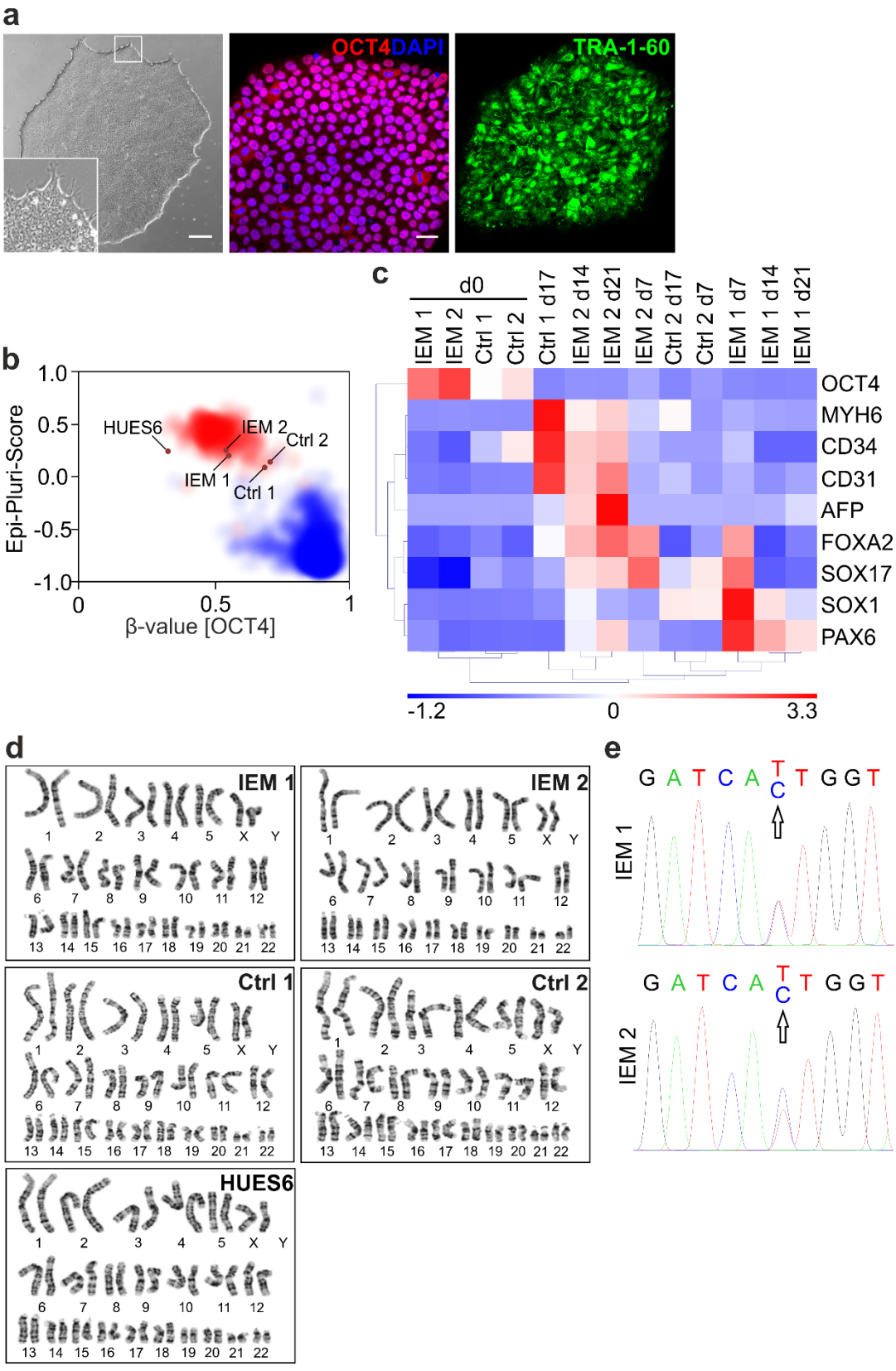

Supplementary Figure S1. IEM specific iPS cells are pluripotent.

(a) Phase contrast and immunofluorescence images of iPS cells from clone IEM 1. iPS cells exhibit an ES cell-like morphology (left) and express the pluripotency

markers OCT4 (red, center) and TRA-1-60 (green, right). Nuclei were counterstained with DAPI (blue). Scale bar 100 µm. Images are representative for all iPS cell clones used. **(b)** DNA methylation levels (β-values) of iPS and HUES6 cells were analyzed at three specific CpG sites located in C14orf115, ANKRD46 and OCT4. Epi-Pluri-Score is calculated as β-value (ANKRD46) – β-value (C14orf115) and plotted versus the β-value of OCT4. The red and blue clouds refer to DNAm profiles (all Illumina HumanMethylation27 BeadChip platform) of 264 pluripotent and 1,951 non-pluripotent cell preparations, respectively [2]. HUES6 and all iPSC lines were clearly classified as pluripotent. **(c)** RT-qPCR results (2^{-dCt} values) of undifferentiated (day 0) and differentiated (day 7, 14, 17 and 21) iPS clones IEM 1, IEM 2, Ctrl 1 and Ctrl 2 were normalized and subjected to bidirectional clustering. Gradation bar represents scale of expression levels: red, high expression; blue, low expression. Pluripotency marker OCT4, ectoderm germ layer SOX1 and PAX6, mesoderm germ layer CD31, CD34, and MYH6 and endoderm germ layer AFP, FOXA2 and SOX17. **(d)** Karyogram showing 22 pairs of autosomal and one pair of sex chromosomes (XX) for IEM 1, IEM 2, Ctrl 1, Ctrl 2 and HUES6 cells. **(e)** Sanger sequencing confirms presence of heterozygous ATT to ACT conversion in codon 848 of Nav1.7 in IEM 1 and IEM 2 leading to an isoleucine to threonine substitution.

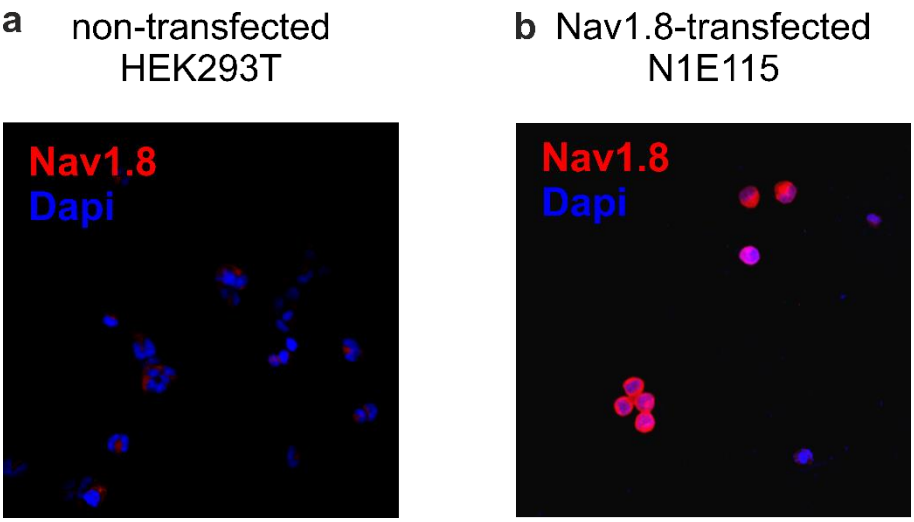

Supplementary Figure S2. Control immunostainings of Nav1.8 antibody.

(a) The Nav1.8 antibody (ASC-016, Alomone Labs, Jerusalem, Israel; dilution 1:1000) was tested in non-transfected HEK293T cells as a negative control and no positive signal could be observed. HEK293T cells were used as they do not express Nav1.8 endogenously. **(b)** The same antibody was used in a 1:1500 dilution on N1E-115 cells, transiently transfected with Nav1.8. The red signal observed in the majority of cells clearly shows Nav1.8-specific staining. Nuclei in both images were counterstained with DAPI (blue). Secondary antibody in both images was goat anti-rabbit IgG Alexa Fluor 594.

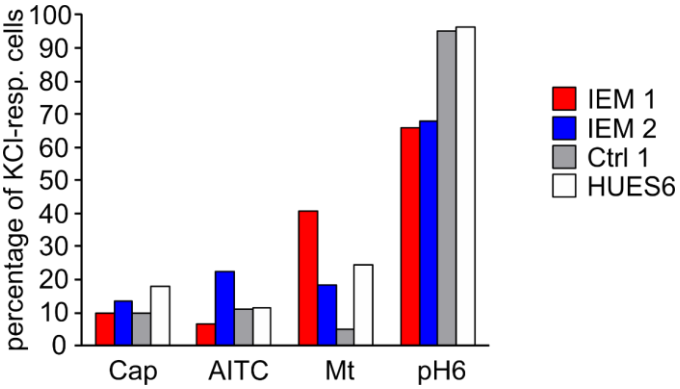

Supplementary Figure S3. Quantification of calcium imaging studies.

Percentage of KCl-responsive iPS cells or HUES-derived neurons responding to stimulation with capsaicin (Cap, 1 µM), AITC (100 µM), menthol (Mt, 100 µM) or pH 6.0 (nKCl = 1232 cells for IEM 1, nKCl = 180 cells for IEM 2, nKCl = 127 cells for Ctrl 1, nKCl = 285 cells for HUES6). No recordings were performed on Ctrl 2. For recording protocol, see Fig. 2e.

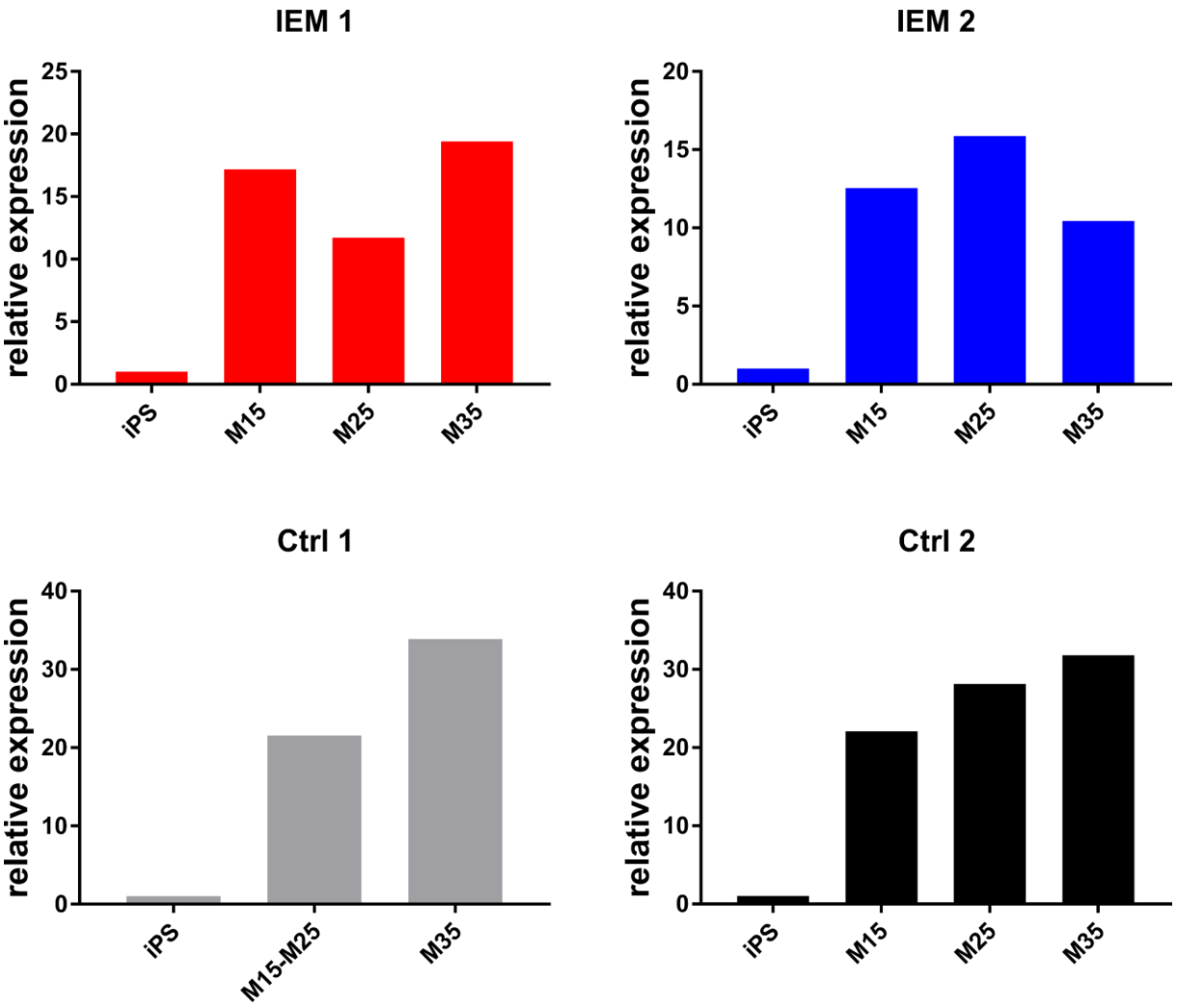

Supplementary Figure S4. Quantification of Nav1.7 mRNA expression using real-time qPCR.

Shown is the relative mRNA expression for Nav1.7. RNA samples were obtained from all four clones at different time points: before differentiation (iPS) and after differentiation at maturation day (M) 15, 25 and 35. Expression of Nav1.7 mRNA at all time points was first normalized to the geometric mean of the expression of mRNA of three housekeeping genes GAPDH, HPRT and B2M. Nav1.7 mRNA levels at the different time points are expressed relative to the level before differentiation (iPS). Nav1.7 mRNA expression is up-regulated during neuronal differentiation.

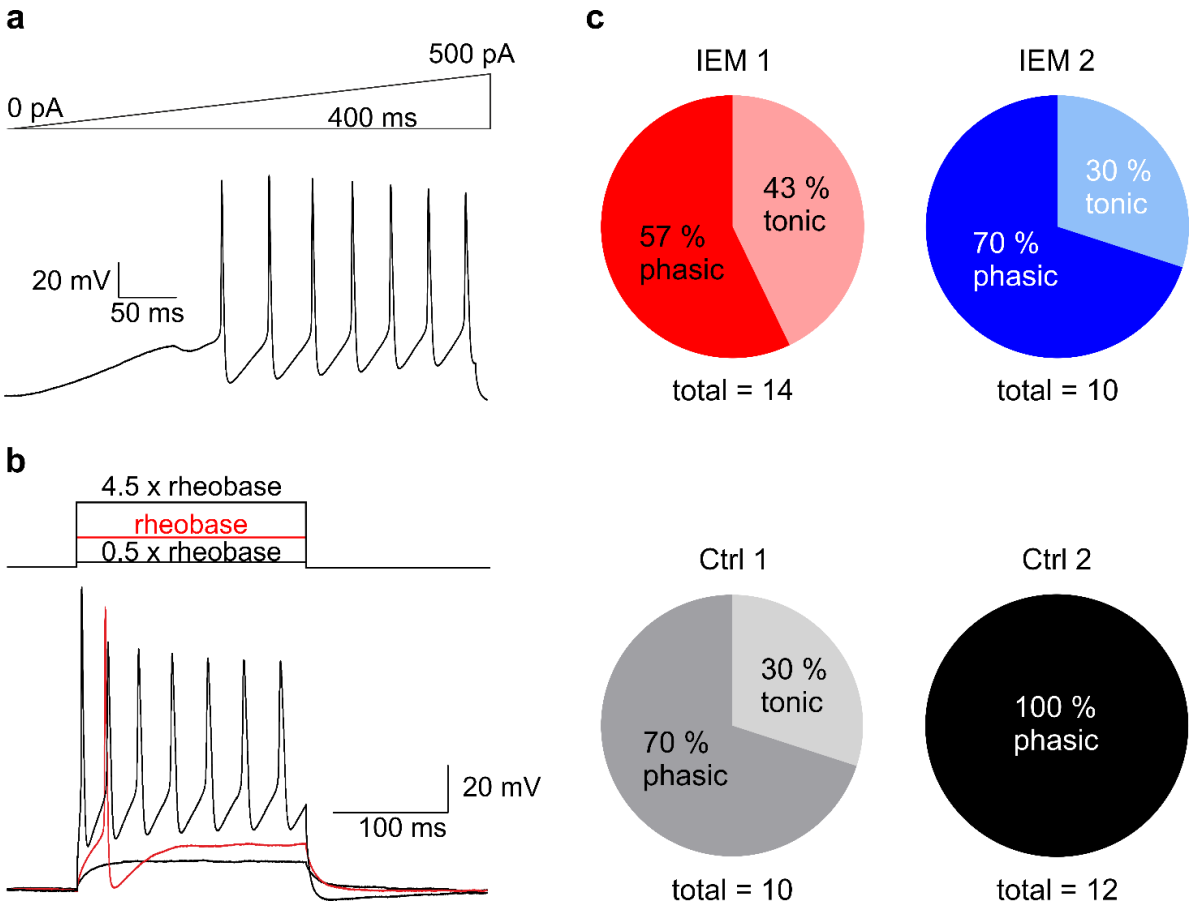

Supplementary Figure S5. IEM-derived nociceptors display tonic action potential firing.

(a) Slow ramp currents (from 0 to 500 pA in 400 ms), starting at a potential of -70 mV, were injected immediately after measuring the RMP of each neuron in order to test for action potential firing. **(b)** Because not all neurons fired action potentials during the slow ramp injection shown in (a), we also applied individually adjusted square current pulses (Δ 0.5 x rheobase) to evoke action potential firing. Neurons were held at a RMP around -70 mV. The figure shows three responses from the same neuron. The trace shown in red displays the first evoked action potential. **(c)** Taking into account action potential responses from ramp (a) or square (b) current injections, we found that 43 % of IEM 1 and 30 % of IEM 2 nociceptors displayed tonic action potential firing, as well as 30 % of Ctrl 1 neurons. However, none of the Ctrl 2 nociceptors displayed tonic action potential firing. Total number of neurons in each condition is indicated.

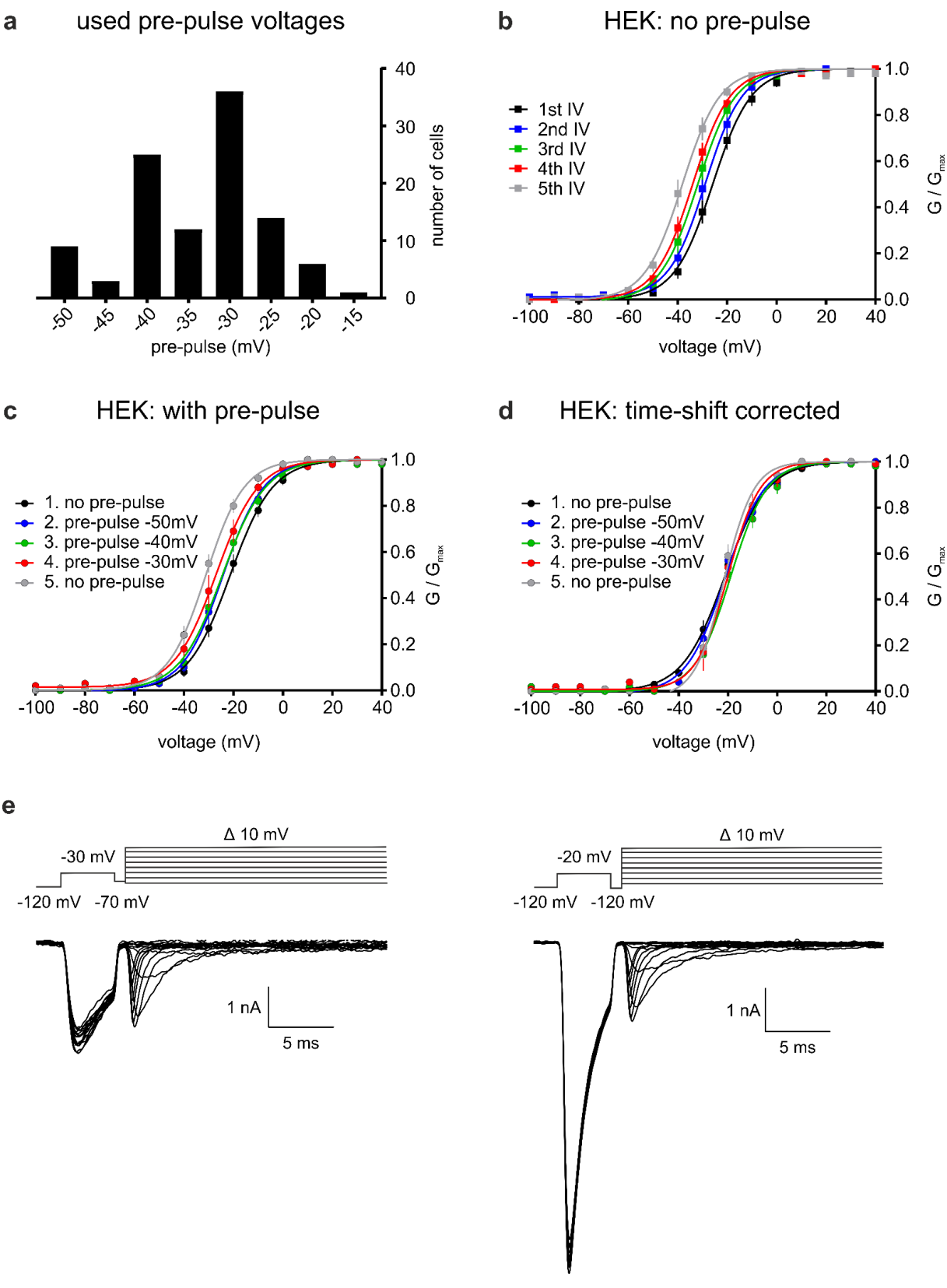
a
used pre-pulse voltages
number of cells
pre-pulse (mV)
b
HEK: no pre-pulse
1st IV
2nd IV
3rd IV
4th IV
5th IV
G / Gmax
voltage (mV)
c
HEK: with pre-pulse
1. no pre-pulse
2. pre-pulse -50mV
3. pre-pulse -40mV
4. pre-pulse -30mV
5. no pre-pulse
G / Gmax
voltage (mV)
d
HEK: time-shift corrected
1. no pre-pulse
2. pre-pulse -50mV
3. pre-pulse -40mV
4. pre-pulse -30mV
5. no pre-pulse
G / Gmax
voltage (mV)
e
Δ 10 mV
-30 mV
-120 mV
-70 mV
1 nA
5 ms
Δ 10 mV
-20 mV
-120 mV
-120 mV
1 nA
5 ms

Supplementary Figure S6. The voltage pre-pulse protocol does not affect activation of Nav1.7

(a) Histogram showing the different pre-pulse voltages that were applied on iPS cell-derived nociceptors of all four clones. The majority of cells were recorded using pre-pulses of -40 mV or -30 mV. **(b)** HEK293 cells, stably expressing WT Nav1.7, were used to measure a sequence of IV curves without pre-pulse (n = 7-11). The calculated activation curves of WT Nav1.7 display a time-dependent hyperpolarized shift. **(c)** HEK293 cells, stably expressing WT Nav1.7, were recorded with different pre-pulses (n = 9-12). The sequence can be seen in the legend and was the same in all cells. Voltage dependence of activation of Nav1.7 displays a similar hyperpolarized shift to control recordings (b). **(d)** The time-dependent shift in the activation of Nav1.7 in (b) was subtracted from recordings in (c). The result shows that the voltage dependence of activation of Nav1.7 is not affected by the pre-pulse protocols. **(e)** An inter-pulse of 1 ms to -120 or -70 mV is sufficient to recover a fraction of Nav1.7 channels and to obtain measurable current amplitudes during the test-pulse in WT Nav1.7-expressing HEK293 cells. The displayed example traces come from two cells with different pre-pulses and inter-pulses.

Supplementary Table S1. PCR primers.

Gene	**Primer sequence (5'-3')**	
Nav1.7	For	TGCTTTACCCTTTGAACAAAAA
	Rev	AAATGCATGAACATCTGGTTACA

Supplementary Table S2. RT-qPCR primer sequences.

Expression of pluripotency and germ layer markers

Gene	Primer sequence (5'-3')		Reference
AFP	For	GCCAAGCTCAGGGTGTAG	
	Rev	CAATGACAGCCTCAAGTTGT	
CD31	For	GAGTCCTGCTGACCCTTCTG	[6]
	Rev	ATTTTGCACCGTCCAGTCC	
CD34	For	TGGACCGCGCTTTGCT	[6]
	Rev	CCCTGGGTAGGTAACTCTGGG	
FOXA2	For	GCATTCCCAATCTTGACACGGTGA	[5]
	Rev	GCCCTTGCAGGCAGAATACACATT	
GAPDH	For	GAAGGTGAAGGTCGGAGTC	[3]
	Rev	GAAGATGGTGATGGGATTTC	
MYH6	For	AAGCTCAAGAACGCCTAC	[1]
	Rev	CATTCTTTCCTCCTTCTCC	
OCT4	For	GGGGGTTCTATTTGGGAAGGTA	[4]
	Rev	ACCCACTTCTGCAGCAAGGG	
PAX6	For	TCGAAGGGCCAAATGGAGAAGAGAAG	[5]
	Rev	GGTGGGTTGTGGAATTGGTTGGTAGA	
SOX1	For	CCTGTGTGTACCCTGGAGTTTCTGT	[5]
	Rev	TGCACGAAGCACCTGCAATAAGATG	
SOX17	For	AGGAAATCCTCAGACTCCTGGGTT	[5]
	Rev	CCCAAACTGTTCAAGTGGCAGACA	

Expression of Nav1.7 channels and housekeeping genes

B2M	For	GCT CGC GCT ACT CTC TCT TT
	Rev	TCT CTG CTG GAT GAC GTG AG
GAPDH	For	AGC CAC ATC GCT CAG ACA C
	Rev	GCC CAA TAC GAC CAA ATC C
HPRT	For	TGA CCT TGA TTT ATT TTG CAT ACC
	Rev	CGA GCA AGA CGT TCA GTC CT
Nav1.7	For	CAC AAT CCC AGC CTC ACA GT
	Rev	CTG AGG AGC TTG ACC GGT TTA

References:

[1] Chen ZQ, Lautenberger JA, Lyons LA, McKenzie L, O'Brien SJ. A human genome map of comparative anchor tagged sequences. J Hered 1999;90:477–484.

[2] Lenz M, Goetzke R, Schenk A, Schubert C, Veeck J, Hemeda H, Koschmieder S, Zenke M, Schuppert A, Wagner W. Epigenetic Biomarker to Support Classification into Pluripotent and Non-Pluripotent Cells. Sci Rep 2015;5. doi:10.1038/srep08973.

[3] Qin J, Li W-Q, Zhang L, Chen F, Liang W-H, Mao FF, Zhang X-M, Lahn BT, Yu W-H, Xiang AP. A stem cell-based tool for small molecule screening in adipogenesis. PloS One 2010;5:e13014.

[4] Tran TH, Wang X, Browne C, Zhang Y, Schinke M, Izumo S, Burcin M. Wnt3a-induced mesoderm formation and cardiomyogenesis in human embryonic stem cells. Stem Cells Dayt Ohio 2009;27:1869–1878.

[5] Yang L, Soonpaa MH, Adler ED, Roepke TK, Kattman SJ, Kennedy M, Henckaerts E, Bonham K, Abbott GW, Linden RM, Field LJ, Keller GM. Human cardiovascular progenitor cells develop from a KDR+ embryonic-stem-cell-derived population. Nature 2008;453:524–528.

[6] Zambidis ET, Peault B, Park TS, Bunz F, Civin CI. Hematopoietic differentiation of human embryonic stem cells progresses through sequential hematoendothelial, primitive, and definitive stages resembling human yolk sac development. Blood 2005;106:860–870.